

The *Caenorhabditis elegans* Skp1-Related Gene Family: Diverse Functions in Cell Proliferation, Morphogenesis, and Meiosis

Sudhir Nayak,¹ Fernando E. Santiago,² Hui Jin,² Debbie Lin,¹ Tim Schedl,¹ and Edward T. Kipreos^{2,3}

¹Department of Genetics
Washington University School of Medicine
St. Louis, Missouri 63110

²Department of Cellular Biology
University of Georgia
Athens, Georgia 30602

Summary

Background: The SCF ubiquitin-ligase complex targets the ubiquitin-mediated degradation of proteins in multiple dynamic cellular processes. A key SCF component is the Skp1 protein that functions within the complex to link the substrate-recognition subunit to a cullin that in turn binds the ubiquitin-conjugating enzyme. In contrast to yeast and humans, *Caenorhabditis elegans* contains multiple expressed Skp1-related (*skr*) genes.

Results: The 21 Skp1-related (*skr*) genes in *C. elegans* form one phylogenetic clade, suggesting that a single ancestral Skp1 gene underwent independent expansion in *C. elegans*. The cellular and developmental functions of the 21 *C. elegans skr* genes were probed by dsRNA-mediated gene inactivation (RNAi). The RNAi phenotypes of the *skr* genes fall into two classes. First, the highly similar *skr-7*, *-8*, *-9*, and *-10* genes are required for posterior body morphogenesis, embryonic and larval development, and cell proliferation. Second, the related *skr-1* and *-2* genes are required for the restraint of cell proliferation, progression through the pachytene stage of meiosis, and the formation of bivalent chromosomes at diakinesis. CUL-1 was found to interact with SKR-1, *-2*, *-3*, *-7*, *-8*, and *-10* in the yeast two-hybrid system. Interestingly, SKR-3 could interact with both CUL-1 and its close paralog CUL-6.

Conclusions: Members of the expanded *skr* gene family in *C. elegans* perform critical functions in regulating cell proliferation, meiosis, and morphogenesis. The finding that multiple SKRs are able to bind cullins suggests an extensive set of combinatorial SCF complexes.

Introduction

The Skp1 gene product was originally identified as a protein that bound the cyclin A/CDK2 complex in conjunction with the F-box protein Skp2 [1]. It was called Skp1, for S-phase kinase-associated protein 1, to denote its association with cyclin A/CDK2. Skp1 was later found to function as a core component of SCF ubiquitin-ligase complexes [2–4]. The SCF complex is a multisubunit ubiquitin-ligase (E3) that facilitates the recognition

of substrates by the ubiquitin-conjugating enzyme (E2) Ubc3/Cdc34 (see [5, 6]).

There are four SCF subunits: Skp1, a cullin (an ortholog of metazoan CUL-1 or budding yeast Cdc53), Rbx1/Roc1/Hrt1, and an F-box protein (see [5, 6]). The cullin subunit acts as a scaffold to link the E2 (Ubc3/Cdc34) to the E3 complex, and this association is facilitated by the Rbx1/Roc1/Hrt1 subunit. The cullin scaffold also binds to Skp1, and Skp1 binds to an F-box protein through a direct interaction with the F-box motif [7]. In the SCF complex, the F-box protein selectively binds phosphorylated substrates to bring them into close proximity to the associated E2 that covalently transfers ubiquitin to the substrate (see [5, 6]). Polyubiquitinated substrates are then subsequently degraded by the 26S proteasome [8].

SCF complexes in yeast and metazoa have been found to target the degradation of a host of proteins, most notably cell cycle regulators and transcription factors (see [5, 6]). Multiple F-box proteins, each with different substrate specificity, can bind the core SCF complex to increase the repertoire of substrates that can be recognized. In yeast, three F-box proteins are known to function in SCF complexes, while, in humans, four F-box proteins have been found to function in SCF complexes [5, 6, 9, 10].

In addition to its roles in SCF complexes, budding yeast Skp1p can associate with F-box and non-F-box proteins to perform cellular functions unrelated to degradation. Skp1p has been found to bind the F-box protein Ctf13p to function in the CBF3 kinetochore complex [11, 12], the F-box protein Rcy1p to facilitate SNARE recycling [13], and the non-F-box protein Rav1p to regulate V-ATPase assembly [14]. These observations indicate that yeast Skp1p can function in diverse molecular and cellular settings.

Here, we present data indicating that the Skp1-related (*skr*) gene family has greatly expanded in *Caenorhabditis elegans* relative to human and yeast genomes, with the *C. elegans* genome containing 21 *skr* genes compared to a single expressed Skp1 gene in fission yeast, budding yeast, and humans. We probed potential interactions with cullins using the two-hybrid system and found that multiple *C. elegans* SKRs have the ability to interact with CUL-1 and that at least one SKR is able to interact with CUL-6, a close paralog of CUL-1. Thus, there is the potential to generate many distinct SCF and SCF-like complexes from combinatorial SKR/CUL interactions. Finally, using RNAi, we have identified roles of the *skr* gene family in regulating multiple cellular processes including restricting cell proliferation, morphogenesis, and meiotic prophase.

Results

Saccharomyces cerevisiae and human Skp1 proteins were used as probes in BLAST searches [15] to identify Skp1 homologs in *S. cerevisiae*, *Schizosaccharomyces*

³Correspondence: ekipreos@cb.uga.edu

pombe, *C. elegans*, *Drosophila melanogaster*, and humans. We identified a single Skp1-related gene in budding yeast and fission yeast. In humans, in addition to the identified Skp1 gene, a number of Skp1 homologs were predicted to exist in other chromosomal locations based on Southern blot analysis [16, 17]. We found that there are at least eight additional Skp1-related genes in the human genome located on chromosomes 4, 5, 7, 9, 10, and 12 (data not shown). However, while the human Skp1 gene is represented in the human EST expression database with 744 entries, there are no EST sequences for any of the other Skp1-related genes, suggesting that they may all in fact be pseudogenes (data not shown). *D. melanogaster* has 6 Skp1 homologs, while *C. elegans* has 21 Skp1 homologs (Figure S1). Members of the elongin C family, which are distantly related to the Skp1 family, were found in all species, suggesting that the ancestral elongin C and Skp1 genes were present prior to the evolutionary divergence of fungi from higher eukaryotes. Elongin C family members were not included in our analysis.

Phylogenetic Analysis of Skp1 and Cullin Homologs

To determine the evolutionary relationships between the multiple *Drosophila* and *C. elegans* Skp1 homologs and the yeast and human Skp1 genes, we performed phylogenetic analyses using neighbor-joining (NJ) and maximum-likelihood (ML) methods [18, 19]. Phylogenetic trees generated by both methods showed that all 21 *C. elegans* Skp1-related genes form one cluster (Figure 1). Similarly, all of the *Drosophila* Skp1 homologs also form a single cluster.

In consultation with K. Nakayama and colleagues, we have named the 21 Skp1 homologs in *C. elegans* “*skr*” for Skp1 related. Six *skr* clades within the *C. elegans* cluster were defined by phylogenetic analysis, and the *skr* genes within each clade were numbered based on similarity to the human and yeast Skp1 homologs (Figure 1 and Table 1). Members of clades were given sequential numbers; the clades most similar to human and yeast Skp1 genes were given lower numbers, and taxa within each clade were also numbered based on similarity.

The *skr* genes are spread over five of the six *C. elegans* chromosomes (Figure 2). The chromosomal location of genes belonging to *skr* clades do not appear to be random and are suggestive of a series of gene duplication events. In three cases, all clade members are found in the same genomic region: the two members of clade I, *skr-1* and *skr-2*, are located within a 2.7-kb region on chromosome I; the three clade VI members, *skr-19*, *skr-20*, and *skr-21*, are located within a 3.7-kb region on chromosome X; and the four members of clade II, *skr-3*–*skr-6*, are all located on the right arm of chromosome V (Figure 2). The close physical association of *skr-1* and *skr-2* and their high degree of sequence identity (83% nucleotide identity, 81% amino acid identity) suggest a recent local duplication event. The close physical association of the members of clade VI also suggests that they were generated by local duplications. In this case, however, sequence identity among the members is low

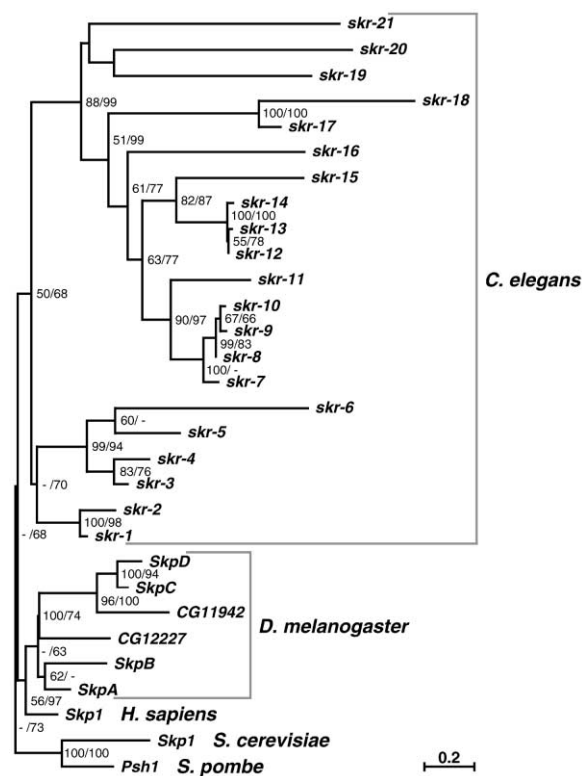


Figure 1. Neighbor-Joining Phylogeny of *H. sapiens*, *S. cerevisiae*, *S. pombe*, *D. melanogaster*, and *C. elegans* Skp1 Family Members. Branch lengths are proportional to the estimated number of amino acid substitutions; the scale bar indicates the estimated amino acid substitutions per site. Bootstrap support values of 50% and above are given at branch nodes and are derived from neighbor-joining (left) and maximum-likelihood (right) analyses, separated by slash marks (dashes indicate scores below 50%). The *C. elegans* and *D. melanogaster* Skp1 homologs are bracketed and labeled.

(46%–49% nucleotide identity, 24%–27% amino acid identity), suggesting either rapid sequence divergence or ancient duplication events.

Interestingly, three members of clade III are found immediately adjacent to members of clade IV (*skr-7* and *skr-14*, *skr-8* and *skr-12*, and *skr-9* and *skr-13*) (Figure 2). In each case, the two genes are oriented away from each other so that the putative promoter regions may be contiguous. The phylogeny suggests that the clades share a common ancestor that underwent duplication to give rise to clades III and IV. The head-to-head orientation of the three paired clade members may therefore be a remnant of an ancestral local inverted duplication that gave rise to the two clades.

C. elegans, *D. melanogaster*, and humans each have six cullin genes, while budding yeast have three (Figures 3 and S2–S4). Phylogenetic analysis reveals that there are five metazoan cullin families (CUL1–CUL5) (Figure 3). *C. elegans*, *Drosophila*, and humans have members of each cullin family. *C. elegans* has two members of the CUL1 family, *cul-1* and *cul-6*; humans have two members of the CUL4 family, *CUL4A* and *CUL4B*; and *Drosophila* has an additional highly diverged cullin, CG11261, that could not be analyzed because its diver-

Table 1. *skr* Genes in *C. elegans*

<i>skr</i> Gene	Cosmid Identification	Clade	Number of ESTs	Two-Hybrid Interaction with Cullins	RNAi Phenotypes
<i>skr-1</i>	F46A9.5	I	12	CUL-1	hyperplasia; early embryo spindle mispositioning, ectopic blebbing, abnormal polar bodies; pachytene arrest; and univalent diakinetid chromosomes
<i>skr-2</i>	F46A9.4	I	5	CUL-1	
<i>skr-3</i>	F44G3.6	II	2	CUL-1, CUL-6	none
<i>skr-4</i>	Y60A3A.18	II	0	ND	none
<i>skr-5</i>	F47H4.10	II	1	none	none
<i>skr-6</i>	Y37H2C.2	II	0	ND	none
<i>skr-7</i>	Y47D7A.1	III	4	CUL-1	late-stage embryo arrest; L1-stage larval arrest with no postembryonic cell division
<i>skr-8</i>	C52D10.9	III	11	CUL-1	and a high percentage of larvae with posterior bulge (kNOB)
<i>skr-9</i>	C52D10.7	III	5	none	
<i>skr-10</i>	Y105C5B.13	III	8	CUL-1	
<i>skr-11</i>	F13A7.9	III	0	ND	none
<i>skr-12</i>	C52D10.6	IV	4	none	none
<i>skr-13</i>	C52D10.8	IV	4	none	none
<i>skr-14</i>	Y47D7A.8	IV	2	none	none
<i>skr-15</i>	F54D10.1	IV	10	none	none
<i>skr-16</i>	C42D4.6	V	0	ND	none
<i>skr-17</i>	C06A8.4	V	1	none	none
<i>skr-18</i>	F56B3.4	V	0	ND	none
<i>skr-19</i>	R12H7.3	VI	4	none	none
<i>skr-20</i>	R12H7.5	VI	2	none	none
<i>skr-21</i>	K08H2.1	VI	5	none	none

gence caused long-branch attraction artifacts in the phylogeny [20]. The *S. cerevisiae cullin C* gene also could not be analyzed due to its high level of sequence divergence.

The *S. cerevisiae cullin B* gene branches at the base of the CUL3 and CUL4 clades with very high bootstrap support values, suggesting that the metazoan *CUL3* and *CUL4* genes arose from a duplication of the ancestral *cullin B* gene. The *S. cerevisiae CDC53* gene branches at the base of the CUL1, CUL2, and CUL5 clades in the NJ phylogeny and within the CUL1 clade in ML analysis (Figure 3, data not shown), suggesting that the CUL1 genes arose from the ancestral *CDC53* gene and possibly CUL2 and CUL5 as well, although the inability to analyze *cullin C* tempers the latter conclusion.

The *C. elegans cul-6* gene appears to have arisen by a duplication of the ancestral *cul-1* gene. This gene duplication event may be specific for nematodes, as counterparts of *cul-6* are not present in *Drosophila* or

humans. Injection of *cul-6* dsRNA to inactivate gene expression (dsRNA-mediated interference, RNAi) [21] produces no phenotype (data not shown). Further, injection of *cul-1(e1756)* heterozygotes with *cul-6* dsRNA did not noticeably affect the hyperplasia phenotype of the homozygous *cul-1* mutant progeny, suggesting that the two genes are not functionally redundant (data not shown).

Interaction of *skr* and Cullin Proteins in the Two-Hybrid System

A total of 16 of the 21 *skr* genes were present as ESTs in the *C. elegans* cDNA Project database, indicating that they are bona fide genes (Table 1). We tested the 16 expressed *skr* genes for interaction with the 6 *C. elegans* cullin genes using the two-hybrid system (Figure 4, Table 1). CUL-1 was able to interact with six of the SKR proteins: SKR-1, SKR-2, SKR-3, SKR-7, SKR-8, and SKR-10. These *skr* genes belong to clades I, II, and III. It is

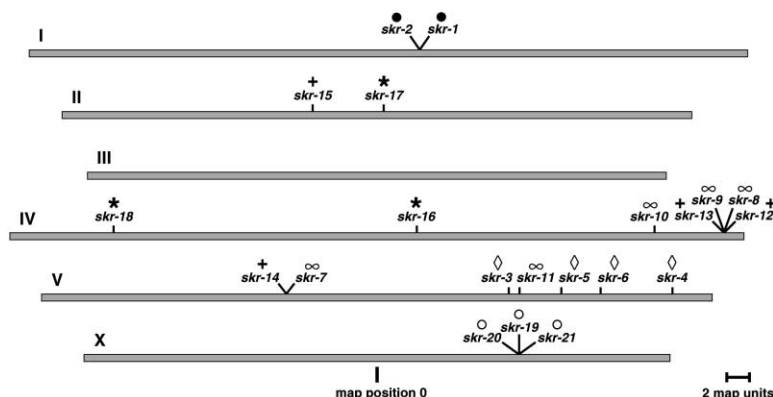


Figure 2. Chromosomal Location of *C. elegans skr* Genes

Bars represent the six *C. elegans* chromosomes. The location of *skr* genes on the chromosomes is based on their genetic map position. Members of clade I are denoted by black dots, members of clade II are denoted by diamonds, members of clade III are denoted by infinity symbols, members of clade IV are denoted by plus symbols, members of clade V are denoted by asterisks, and members of clade VI are denoted by open circles. Genetic map position 0 is denoted at the bottom; positions to the left of this are negative map positions, and positions to the right are positive map positions.

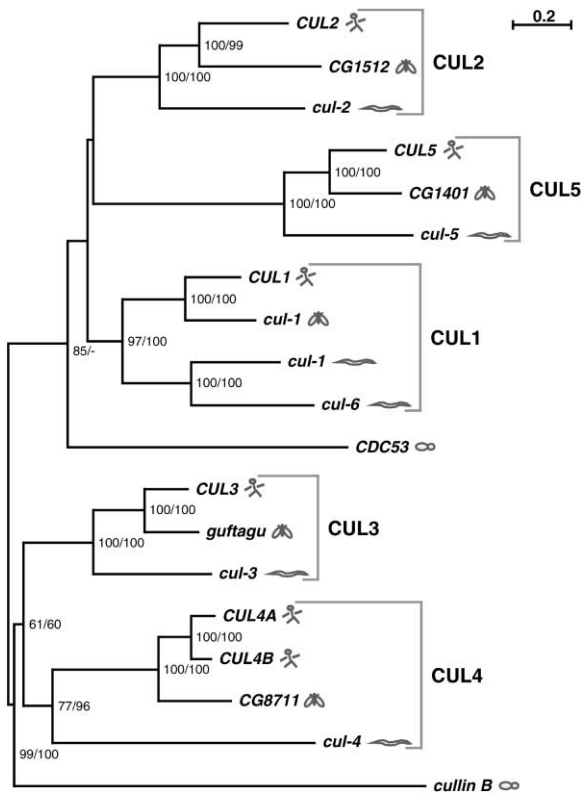


Figure 3. Neighbor-Joining Phylogeny of *H. sapiens*, *S. cerevisiae*, *D. melanogaster*, and *C. elegans* Cullin Family Members. Branch lengths and bootstrap values are the same as described in Figure 2. Species are denoted by cartoon. The *D. melanogaster* cullin *CG11261* and *S. cerevisiae* cullin *C* were not included in the analysis because their high level of sequence divergence caused long-branch attraction artifacts [20].

intriguing that we did not detect interaction between SKR-9 and CUL-1, as SKR-9 is highly related to SKR-7, SKR-8, and SKR-10, sharing 86%–96% amino acid identity with the three proteins. Interaction between the SKRs and CUL-2, CUL-3, CUL-4, and CUL-5 was not observed. CUL-6, in contrast, was able to interact with SKR-3 in the two-hybrid system.

Loss-of-Function Phenotypes of *skr-7*, *skr-8*, *skr-9*, and *skr-10*

To define the function of the *C. elegans skr* genes, we used the rapid and highly selective method of dsRNA-mediated interference (RNAi) [21]. We performed RNAi analysis on the 21 *skr* genes and found that 6 of the genes, falling in clades I and III, produced 2 distinct classes of phenotypes (Table 1) that are detailed below. The remaining 15 genes did not produce detectable RNAi phenotypes. To attempt to uncover redundant phenotypes within clades, we injected double and triple combinations of dsRNA. The following combinations of dsRNA were tested: *skr-3/skr-4*, *skr-5/skr-6*, *skr-12/skr-13*, *skr-13/skr-14*, *skr-12/skr-15*, *skr-17/skr-18*, *skr-19/skr-20*, and *skr-19/skr-20/skr-21*. None of these combination injections produced obvious phenotypes by RNAi. The injection of more than three dsRNAs was not

attempted, as it has been reported to reduce the overall effectiveness of the procedure [22].

Four members of clade III, *skr-7*, *skr-8*, *skr-9*, and *skr-10*, produced similar embryonic and larval RNAi phenotypes. The percentage of progeny that arrested as embryos varied depending on the efficacy of injections and ranged from ~5%–~50%. The embryos arrested with a completely formed pharynx and variable amounts of elongation (data not shown). The progeny that hatched arrested in the L1 larval stage, with no postembryonic cell divisions by the larval blast cells (cell divisions were scored from $n = 5$, $n = 3$, $n = 8$, and $n = 3$ animals following RNAi of *skr-7*, *-8*, *-9*, and *-10*, respectively). A large percentage of the L1-arrested larvae (40%–87%) had a posterior kNOB of disorganized tissue and often had shorter posterior body length (NOB-phenotype) (Figure 5A). In these animals, cell identification was problematic because of the disorganized morphology; however, there did not appear to be any postembryonic divisions.

The genes *skr-7*, *skr-8*, *skr-9*, and *skr-10* are highly homologous with 82% of nucleotide positions identical across an alignment of all four genes. This level of homology is predicted to produce cross-RNAi inactivation, so that injection of dsRNA for one of these genes would lead to the inactivation of all of them [23]. Therefore, the phenotypes described for this gene group could be due to the inactivation of a single *skr* gene or to the inactivation of combinations of redundant *skrs*. The fifth member of clade III, *skr-11*, which has no RNAi phenotype, is significantly more divergent and does not have large stretches of perfect nucleotide sequence identity with the other four clade members that would trigger cross-RNAi inactivation.

To probe whether there were redundant phenotypes that were not revealed by the predicted cross-RNAi, we coinjected dsRNA for *skr-7* and *skr-9* dsRNA in an attempt to ensure the inactivation of the entire clade. This double injection provided 98% nucleotide identity coverage for the set of all four genes. We used the percentage of embryonic arrest as an indicator of the severity of the RNAi phenotype. Injection of *skr-7* dsRNA alone produced 53% arrested embryos, *skr-9* dsRNA alone gave 20% arrested embryos, while injection of the double combination *skr-7* and *skr-9* gave a value in between the single RNAi injections (44% arrested embryos). In all cases, the embryonic and larval RNAi phenotypes appeared similar. These results indicate that targeting additional members of *skr-7*–*skr-10* for RNAi does not reveal additional phenotypes.

Loss-of-Function Phenotypes of *skr-1* and *skr-2*

The sole members of clade I, *skr-1* and *skr-2*, share 83% nucleotide identity, which is also predicted to produce cross-RNAi effects. RNAi of each gene singly or both genes together resulted in identical phenotypes, and we therefore refer to them in the text as *skr-1/2*. The analysis of *skr-1/2* RNAi phenotypes was performed in two phenotypic windows: 0–16 hr and >16 hr postinjection.

A phenotype of larval hyperplasia of the somatic gonad and hypodermis is observed in a percentage of the initial progeny of wild-type hermaphrodites injected with

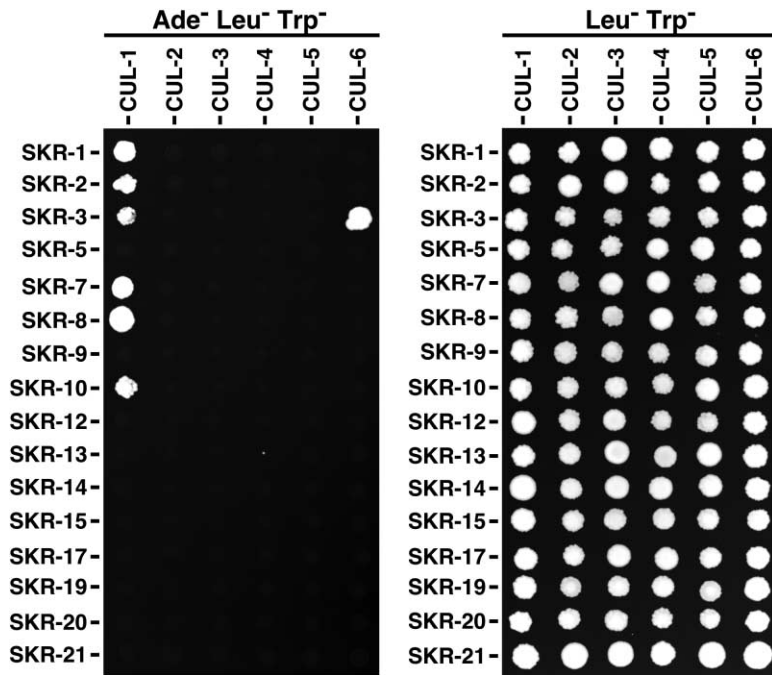


Figure 4. Two-Hybrid Interaction between SKR and Cullin Proteins

pJ69-4A yeast cotransformed with the indicated *skr*/pACTII two-hybrid expression plasmid (denoted by row) and the indicated cullin/pAS1-CYH2 plasmid (denoted by column) were spotted at a density of approximately 200 cells/spot on media deficient for leucine, tryptophan, and adenine to test for interaction between the SKR and cullin proteins (left), and media deficient for leucine and tryptophan that merely selects for the presence of both plasmids (right). Similar results were obtained for growth on histidine-deficient plates (data not shown).

skr-1 or *skr-2* dsRNA (0–16 hr postinjection) (Figures 5B and 5C; data not shown). The phenotype of *skr-1/2* RNAi for all embryos laid after 16 hr postinjection is embryonic arrest. The *skr-1/2* RNAi embryos arrest with a large number of cells but no overt morphogenesis. Nuclear counts of confocal sections revealed that both *skr-1* and *skr-2* have excessive cell numbers, with almost twice the terminal number found in wild-type embryos (Figures 5D–5F). Wild-type embryos hatch with 558 cells [24], while *skr-1* embryos arrest with 863 ± 46 cells ($n = 5$) and *skr-2* embryos arrest with 1010 ± 94 cells ($n = 5$). This embryonic hyperplasia is similar to that seen in

embryos lacking *cul-1* [25]. These observations indicate that *skr-1/2* are required to restrain cell proliferation in both embryonic and larval stages.

It is likely that *skr-1* and *skr-2* maternal products are provided to embryos, as both genes are enriched in the germline and in early embryos [26–28]. The presumed reason that progeny from 0–16 hr post-*skr-1/2* dsRNA injection can develop normally through embryogenesis while progeny obtained >16 hr postinjection have an embryonic phenotype is that injection of dsRNA causes the degradation of *skr-1/2* mRNA transcripts in the germline and embryos but has no effect on already pro-

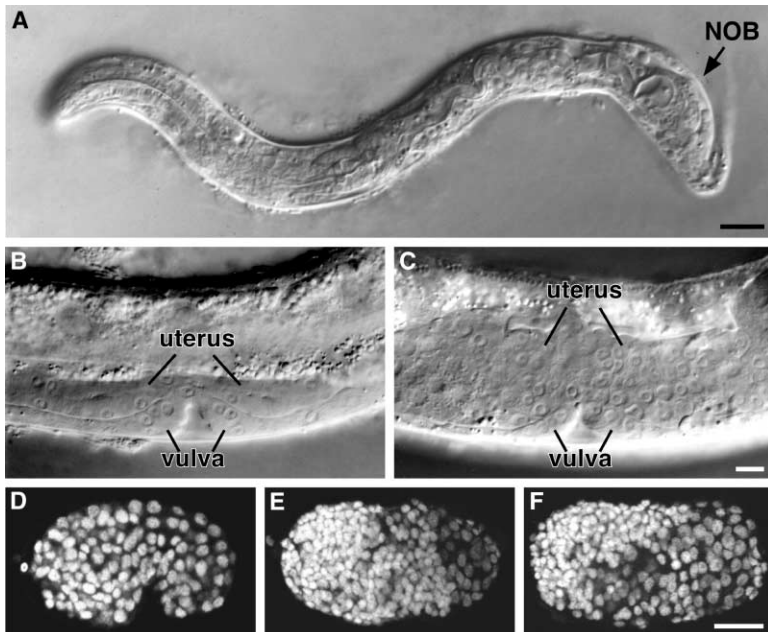


Figure 5. RNAi Phenotype of *skr* Genes

(A) DIC image of *skr-8* RNAi L1-stage-arrested larvae. The posterior bulge (NOB phenotype) is noted (NOB).

(B and C) DIC images of the vulva and uterus of (B) wild-type and (C) *skr-1* RNAi L4-stage larvae. Note the uterine hyperplasia in the *skr-1* RNAi animal.

(D–F) Confocal sections of DAPI-stained (D) wild-type comma-stage embryo, (E) *skr-2* RNAi-arrested embryo, and (F) *skr-1* RNAi-arrested embryo. At the comma stage, wild-type embryos have completed the vast majority of their embryonic cell divisions, and the small number of subsequent cell divisions are balanced by programmed cell deaths [24]. Note the excess cell numbers in the *skr-1* and *skr-2* embryos.

duced maternal proteins. While maternal protein is available, progeny can develop through embryogenesis normally but then manifest phenotypes associated with loss of zygotic message during larval development. As maternal protein becomes depleted in the germline of the injected parental hermaphrodite, embryonic phenotypes become apparent in the progeny.

skr-1 and *skr-2* RNAi embryos also show three defects during early embryonic divisions: a mispositioning of the P₀ spindle so that the daughter cell AB is often not significantly larger than the P1 cell, abnormally shaped or missing polar bodies, and blebbing/ectopic furrows. The blebbing/ectopic furrows occur predominantly in the AB cell and in AB descendents and start immediately after mitosis and last until a few minutes before the next mitosis. These early embryonic phenotypes were also observed for *skr-1* RNAi by Piano et al. as part of a screen to describe the early embryonic phenotypes of germline-expressed cDNAs [27]. The *skr-1/2* early embryonic defects are not expected to lead to hyperplasia in the embryo, as RNAi of other genes can produce embryos with similar early embryonic defects that do not later develop hyperplasia [29, 30].

***skr-1/2* Zygotic RNAi Results in Sterility, but Not Embryonic Lethality**

As an alternative method to examine the postembryonic phenotypes associated with reduction of *skr-1* and *skr-2* function, we took advantage of the RNAi-resistant strain *rde-1(ne300)* [31] to produce progeny that had *skr-1/2* maternal product but would lose *skr-1/2* expression during larval and adult development, an approach termed “zygotic RNAi” (see the Supplementary Material available with this article online). *rde-1(ne300)* hermaphrodites were injected with *skr-1* or *skr-2* dsRNA and were mated with wild-type males, and cross progeny were examined for phenotypes. The RNAi resistance conferred by the *rde-1(ne300)* mutant mothers allows maternal *skr-1/2* mRNAs to persist, permitting normal development beyond the early embryonic lethality associated with *skr-1/2* depletion. In contrast to *skr-1/2* RNAi in a wild-type background, zygotic RNAi resulted in *skr-1/2*(RNAi); *rde-1/+* progeny that were able to grow to adulthood without any obvious abnormalities in somatic tissues, potentially due to a longer delay in the onset of the RNAi effect. The resulting adult hermaphrodites, however, were sterile with >90% penetrance (70/75 animals).

***skr-1/2* RNAi Results in Pachytene Arrest during Female Meiosis**

To determine the nature of the sterile hermaphrodite phenotype resulting from *skr-1/2* zygotic RNAi, gonad arms were dissected and stained with DAPI to visualize nuclear morphology. Control zygotic RNAi using GFP (green fluorescent protein) dsRNA yielded hermaphrodite gonad arms that were morphologically identical to wild-type, with normal distal-to-proximal polarity where zones characteristic of germline development were clearly evident (i.e., mitotic, transition, pachytene, diaki-

nesis/late-stage oogenesis) (60/60) (Figure 6A, top). The nuclei of germ cells entering meiosis in the transition zone have a crescent-shaped morphology; while, in the subsequent pachytene stage of meiotic prophase, nuclei take on a characteristic “thread-like” morphology (Figure 6A, top, insert). In the final diplotene/diakinesis stage in the proximal gonad, oocytes enlarge and become more fully cellularized. Oocytes in diakinesis are large cells containing six highly condensed bivalents (Figure 6A, top, oocytes). In hermaphrodites, the first 40 germ cells that progress through meiosis during the L4 stage differentiate into sperm, and all subsequent germ cells that progress through meiosis make oocytes.

The *skr-1/2* zygotic RNAi germlines exhibit three major defects: an arrest in pachytene with a failure of germ cells to progress to diplotene/diakinesis, an expanded transition zone, and the presence of “gaps” in the gonad arm. In wild-type and control zygotic RNAi adult animals, germ cells with pachytene morphology are never observed after the loop region (Figure 6A, top). In *skr-1/2* RNAi adults, germ cells with thread-like nuclear morphology, indicative of the pachytene stage of meiosis, were observed extending to the far proximal end of the gonad arm (Figure 6A, bottom, insert). *skr-1/2* RNAi gonads also had an expanded transition zone containing nuclei that appeared morphologically normal with the characteristic crescent-shaped nuclear morphology. Additionally, the density of nuclei in the transition zone and pachytene was reduced relative to wild-type, and, in all cases (253/253 arms), small regions or gaps were observed that were devoid of germline nuclei. The gaps were more frequent proximal to the loop and became more pronounced in older animals. The mitotic zone in *skr-1/2* RNAi arms appeared similar to wild-type (100%; 253/253 arms) (Figure 6A, bottom).

To further characterize the developmental stage of the arrested germ cells, we examined the accumulation of two germline markers, GLD-1 and HIM-3 [32, 33]. GLD-1 is a cytoplasmic KH motif RNA binding protein. During female meiotic development, GLD-1 levels are maximal during the pachytene stage and then abruptly fall in the loop as germ cells progress to diplotene and undergo late stages of oogenesis (Figure 6B, top). HIM-3 is a meiosis-specific axial element protein that localizes to synapsed chromosomes beginning in leptotene of meiotic prophase [33].

skr-1/2 zygotic RNAi germlines showed expanded GLD-1 accumulation extending to the far proximal region, encompassing all of the cells with pachytene morphology (Figure 6B, bottom). This result supports the conclusion that *skr-1/2* zygotic RNAi germ cells are arrested in pachytene. HIM-3 staining appeared normal in *skr-1/2* zygotic RNAi germlines (data not shown), indicating that germ cells begin meiotic development at the appropriate position and that at least some aspects of meiotic chromosome structure are normal.

A small fraction of *skr-1/2* zygotic RNAi gonad arms (16%; 31/192 arms) showed signs of progression past pachytene with the presence of diakinetically nuclei and late-stage oocytes. Interestingly, many of the diakinetically oocytes contained exclusively univalent chromosomes (31%; 19/62 oocytes), and all of the remaining oocytes contained at least one univalent compared to wild-type

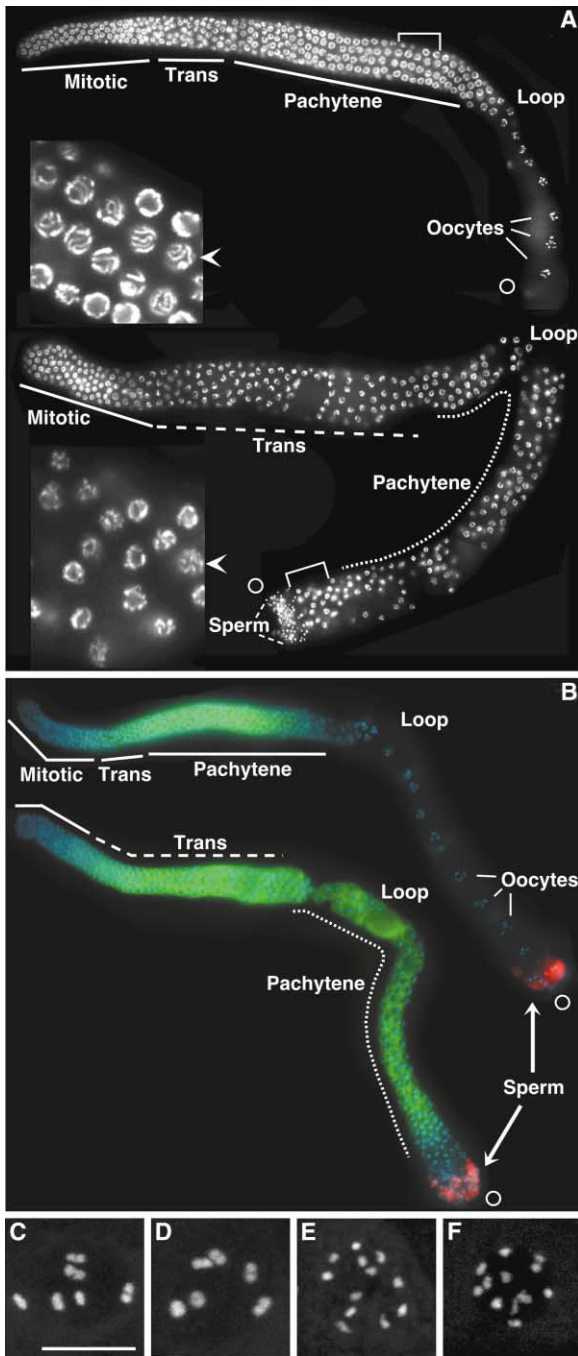


Figure 6. Germline Phenotypes Following *skr-1/2* RNAi
(A) Comparison of zygotic RNAi phenotype following injection of GFP dsRNA (top) and *skr-2* dsRNA (bottom). Dissected gonad arms were stained with DAPI to visualize germline DNA morphology in adult hermaphrodites 48 hr past the L4 stage. The GFP RNAi phenotype (top) is indistinguishable from wild-type, while *skr-2*(RNAi) (bottom) produce sperm, then pachytene-arrested nuclei. The mitotic, transition (trans), and pachytene regions of the germlines are indicated [49]. The proximal end of each gonad arm is indicated by an open circle. A higher-magnification view of the pachytene regions indicated by the brackets is shown in the insets, with representative nuclei denoted by an arrow. In *skr-2*(RNAi) germlines, the transition and pachytene regions are greatly expanded, and the boundary between these regions is difficult to define, as the pachytene mor-

phology is abnormal. Gaps in the *skr-2*(RNAi) germline that are devoid of nuclei are observed.

(B) GLD-1 and SP56 accumulation in control and *skr-1/2* zygotic RNAi gonad arms. Dissected gonad arms were stained with DAPI (blue) and anti-GLD-1 (green) to visualize germ cells in female meiotic prophase through pachytene [32] and with anti-SP56 (red) to identify spermatogenic germ cells [34]. Dashed lines indicate the expanded transition and pachytene regions for *skr-1/2* RNAi animals. GLD-1 staining in control animals (top, green) diminishes rapidly in the loop region in which germline nuclei progress from pachytene to diplotene and is not detectable in the proximal region that contains oocytes in diakinesis. In contrast, GLD-1 levels in *skr-1/2* RNAi germlines (bottom, green) remain high to the far proximal region encompassing all cells that appear to be arrested in pachytene. RME-2, a marker for late-stage oocytes in diplotene/diakinesis [50], fails to accumulate in *skr-1/2* RNAi germlines (data not shown). Spermatogenesis is not obviously affected in *skr-1/2* animals (sperm, red SP56).

Discussion

Skp1 and Cullin Gene Families in *C. elegans*

The Skp1-related (*skr*) gene family is greatly expanded in *C. elegans* (with 21 members) and to a lesser extent in *Drosophila* (with six members). Phylogenetic analysis indicated that all 21 *C. elegans skr* genes form one cluster and all *Drosophila skr* homologs also form a single cluster. These results suggest that a single ancestral Skp1 gene underwent independent expansions in the insect and nematode lineages. In marked contrast, budding yeast, fission yeast, and human genomes each contain only a single expressed Skp1 gene.

The first functions to be defined for Skp1 proteins were in the context of SCF ubiquitin-ligase complexes, where they function to link substrate binding F-box proteins to the core SCF complex [5, 6]. It is interesting that, in addition to the dramatic increase in Skp1 homologs

(C–F) Two-dimensional projections of three-dimensional series of confocal sections of DAPI-stained diakinetive chromosomes for wild-type (C) and P₀ wild-type hermaphrodites injected with (D) *cul-1* dsRNA, (E) *skr-1* dsRNA, and (F) *skr-2* dsRNA. Note that the characteristic 6 “dumbbell”-shaped bivalents have separated to 12 univalents in the oocytes of *skr-1/2* dsRNA-injected animals. The scale bar represents 10 μm.

in *C. elegans*, there has been an even more extensive expansion in the number of genes encoding F-box proteins. *C. elegans* is predicted to contain a remarkable 326 predicted F-box protein genes; in contrast, there are 11 F-box protein genes in budding yeast, 22 in *Drosophila*, and approximately 40 in humans (see [36]). In contrast to Skp1 and F-box protein genes, the cullin gene family is very stable throughout metazoa, with five major cullin paralogs present in nematodes, flies, and mammals. Human Skp1 was found to bind to CUL1, but not to other cullins [37]. Interestingly, in the context of the expansion of Skp1 and F-box protein genes in *C. elegans*, there has also been an apparent nematode-specific duplication within the *C. elegans* CUL1 clade to produce two genes, *cul-1* and *cul-6*.

We show that at least six SKR proteins (SKR-1, SKR-2, SKR-3, SKR-7, SKR-8, and SKR-10) can interact with CUL-1. SKR-3 can also bind CUL-6, indicating that CUL-6 may function in SCF complexes, thereby further expanding the potential number of core SCF complexes in *C. elegans* to seven. Core SCF complexes in yeast and humans bind multiple F-box proteins to increase the number of substrates that can be recognized [5, 6]. Given the potential for at least seven different core SCF complexes and the dramatic expansion in the number of F-box proteins, there may be a vast array of distinct SCF complexes in *C. elegans*.

Diverse SKR-1/SKR-2 Functions in Mitotic Cell Proliferation and Meiosis

The SKR-1 and SKR-2 proteins were found to interact with CUL-1. The two genes are very similar and are likely subject to cross-RNAi effects, making redundancy of function difficult to ascertain. The RNAi phenotype for the two genes includes embryonic and larval hyperplasia similar to CUL-1, suggesting that they function with CUL-1 in an SCF complex. The F-box protein LIN-23 also has a hyperplasia mutant phenotype [36]. LIN-23 is capable of interacting with both SKR-1 and SKR-2 in the two-hybrid system (data not shown), suggesting that SCF^{LIN-23} complexes containing CUL-1, LIN-23, and either SKR-1 or SKR-2 function to promote cell cycle exit during *C. elegans* development.

In addition to the hyperplasia phenotype, *skr-1/2* have other RNAi phenotypes: early embryonic defects, an arrest in female meiotic pachytene, and oocytes containing univalent diakinetid chromosomes. The latter two *skr-1/2* phenotypes are observed by both zygotic RNAi and in the germline of injected P₀ animals. In contrast, these two phenotypes are not observed in *cul-1* null mutants, in zygotic RNAi of *cul-1*, or in the germline of P₀ animals injected with *cul-1* dsRNA. However, *cul-1* null mutants arrest in the L3 and L4 larval stages and so do not progress to the point at which female meiotic phenotypes would manifest [25], and RNAi may not be sufficient to reveal the full spectrum of *cul-1* phenotypes.

skr-1/2 RNAi produces a number of early embryonic defects, most notably, abnormally shaped or missing polar bodies, mispositioning of mitotic spindles, and ectopic blebbing. Interestingly, these phenotypes are also observed upon inactivation of *cul-2* [30]. However, *cul-2* RNAi or homozygous null mutant embryos have

additional defects that are not observed in *skr-1/2* RNAi embryos: the presence of multiple nuclei in most cells, presumably due to an inability to condense mitotic chromosomes; a dramatic lengthening of the time spent in mitosis; and an early embryonic arrest with, on average, only 24 cells (4% of the wild-type number at hatch) [30].

The array of germline phenotypes indicates that *skr-1/2* may have multiple functions in female meiotic development. Pachytene arrest, an expanded transition zone, and regions of the gonad that are devoid of germ cells were the predominant characteristics of *skr-1/2* zygotic RNAi hermaphrodites, while univalent chromosomes at diakinesis were observed in the remaining hermaphrodites in which meiotic development and gametogenesis progressed past pachytene. Pachytene arrest phenotypes in *C. elegans* have been observed in four other settings. Mutations in the RAS/MAP kinase signaling pathway, including the genes *mek-2*, *mpk-1*, and *let-60*, result in pachytene arrest with a distinctive nuclear-clumping phenotype [38]. Certain *gld-1* alleles, or *gld-1* mutant combinations, give rise to an oogenesis-specific pachytene arrest phenotype [39, 40]. Mutation of *daz-1*, which encodes an RRM-type RNA binding protein similar to a putative human azoospermia factor, has an oogenesis-specific pachytene arrest phenotype [41]. Finally, RNAi of the importin α gene *ima-3* causes a pachytene-like arrest phenotype with abnormal chromosome morphology [42]. While all of these mutants share the pachytene arrest phenotype with *skr-1/2* RNAi, there are differences between *skr-1/2* RNAi and each of these mutants in arrest morphology and/or other germline phenotypes so that none entirely match the *skr-1/2* RNAi germline phenotype.

A failure in pairing, synapsis, or recombination can lead to univalent/achiasmatic chromosomes in diakinetid oocytes [33, 43, 44]. Mutations in *chk-2*, the *C. elegans* homolog of the *Cds1/Chk2* checkpoint protein kinase, result in a failure of pairing between homologous chromosomes and generate univalent/achiasmatic chromosomes at diakinesis [43]. Mutation of *spo-11*, the *C. elegans* homolog of the yeast double-stranded break-generating enzyme that functions in the initiation of meiotic recombination, also leads to univalent/achiasmatic chromosomes at diakinesis [44]. However, despite the failures in pairing and/or recombination, the progression of nuclei through meiotic prophase to diakinesis and gametogenesis is normal in *chk-1* and *spo-11* mutants. Thus, *skr-1/2* may have two separate meiotic functions: one, presumably in pairing, synapsis, or recombination, for the generation or maintenance of bivalent chromosomes at diakinesis; and a second function that is required for pachytene progression and gametogenesis.

SKR-7, -8, -9, and -10 Function to Promote Cell Proliferation and Posterior Morphogenesis

RNAi for *skr-7*, *-8*, *-9*, and *-10* individually resulted in similar phenotypes of early larval arrest with no cell division, embryonic arrest without excessive cell numbers, and a posterior morphogenesis defect. However, due to the extensive stretches of nucleotide sequence identity among these genes, RNAi for one member is likely to inactivate all four genes [23]. Therefore, it is

currently not known if these genes (or a subset) act redundantly or singly in the specific cellular functions implied by the RNAi phenotypes.

SKR-7, -8, and -10 have the capability to interact with CUL-1; however, their RNAi phenotypes are not observed in *cul-1* mutants or *cul-1* RNAi animals. Homozygous *cul-1* mutant progeny of heterozygous parents have normal embryonic and L1-stage development due to the perdurance of maternal product [25]. All subsequent divisions of larval blast cells produce excessive cell numbers due to a failure of dividing cells to exit the cell cycle [25]. The *skr-7*, -8, -9, and -10 RNAi phenotypes of early larval arrest with no cell division suggests that larval blast cells do not enter the cell cycle in the absence of SKR-7, -8, -9, and -10 activity. In contrast, *cul-1* mutants have normal cell cycle entry [25]. Similarly, the posterior morphogenesis defect seen in *skr-7*, -8, -9, and -10 RNAi larvae is not visible in *cul-1* mutants or *cul-1* RNAi animals. The fact that the *skr-7*, -8, -9, and -10 phenotypes are not seen in animals that completely lack CUL-1 activity suggests that CUL-1 is not required for these processes. This suggests that SKR-7, -8, -9, and -10 are likely to carry out at least some of their functions independently of SCF complexes.

The majority of tested SKR proteins did not interact with any *C. elegans* cullins in the two-hybrid system. However, the caveat exists that real but relatively weak interactions may not be detected with the two-hybrid system. A majority of *skr* genes (15/21) also did not produce observable RNAi phenotypes. There are three major reasons why we may not have observed loss-of-function phenotypes for genes that have important physiological roles in *C. elegans*. First, certain *skr* genes may be resistant to RNAi or function in a tissue known to be partially refractory to RNAi, such as in neurons [45]. Second, the presence of subtle, conditional, behavioral, or stage-specific (such as dauer) phenotypes may not have been observed under the conditions used. Finally, a given *skr* gene, or genes, may function redundantly with other cellular pathways so that animals appear wild-type even with severe reduction of gene function. Deciphering the function of many of these *skr* genes may require alternative approaches, such as protein-interaction mapping.

Conclusions

We have demonstrated that two groups of related *skr* genes in *C. elegans* have RNAi phenotypes that indicate multiple roles in development, including positive and negative regulation of cell proliferation, morphogenesis of the posterior body, and central aspects of female meiotic development. Six SKRs could interact with CUL-1, one of which could also interact with CUL-6. This indicates that *C. elegans* is likely to have multiple core SCF complexes.

Experimental Procedures

Phylogenetic Analysis

Alignments of Skp1 and cullin protein sequences were made with CLUSTAL X [46]. The alignments were then optimized by hand to minimize insertions/deletions (Figures S1–S4). Neighbor-joining (NJ) and maximum-likelihood (ML) methods employing Dayhoff and JTT

amino acid substitution models were used to create phylogenies (see the Supplementary Material).

Molecular Analysis

A total of 16 *skr* cDNAs were obtained from the *C. elegans* EST project and were sequenced. GenBank accession numbers are: *skr-1* (AF440505), *skr-2* (AF440506), *skr-3* (AF440507), *skr-5* (AF440508), *skr-7* (AF440509), *skr-8* (AF440510), *skr-9* (AF440511), *skr-10* (AF440512), *skr-12* (AF440513), *skr-13* (AF440514), *skr-14* (AF440515), *skr-15* (AF440516), *skr-17* (AF440517), *skr-19* (AF440518), *skr-20* (AF440519), and *skr-21* (AF440520).

Two-hybrid analysis was performed with *skr* genes in the pACTII (activation domain) vector and with cullin genes in the pAS1-CYH2 (DNA binding domain) vector (Clontech). All *skr* and cullin genes used in the two-hybrid analysis encode full-length protein products, except for *skr-14*, which is missing the first 70 bp of the predicted sequence. Transformation of the *S. cerevisiae* strain pJ69-4A [47] was performed as described [48]. Interaction in the two-hybrid system was tested by growth on both histidine- and adenine-deficient selective media, as well as for β -galactosidase activity.

RNA-Mediated Interference (RNAi)

skr cDNAs were used as templates to make dsRNA when available. For the five *skr* genes without cDNAs, we used genomic DNA as the template, with primers extended approximately 100 bp beyond the predicted 5' and 3' end of the genes. The presence of developmental defects was assessed by stereo and differential interference contrast (DIC) microscopy. A detailed description of zygotic RNAi as well as methods for immunofluorescence and confocal microscopy are available in the Supplementary Material.

Supplementary Material

Supplementary Material including two figures and additional methodological detail is available at <http://images.cellpress.com/supmat/supmatin.htm>.

Acknowledgments

We would like to thank Yuji Kohara and the *C. elegans* EST project for providing cDNA clones, B. Grant and D. Hirsh for generously providing the anti-RME-2 antibody, Monique Zetka for providing the anti-HIM-3 antibody, and SiQun Xu for injections. This work was supported by grants from the National Institutes of Health (GM55297) and the Human Frontier Science Program (RG-229/98) to E.T.K. and National Institutes of Health grant GM63310 to T.S. S.N. is supported by National Institutes of Health post-doctoral fellowship GM20864.

Received: November 19, 2001

Revised: January 7, 2002

Accepted: January 7, 2002

Published: February 19, 2002

References

1. Zhang, H., Kobayashi, R., Galaktionov, K., and Beach, D. (1995). p19^{Skp1} and p45^{Skp2} are essential elements of the cyclin A-CDK2 S phase kinase. *Cell* 82, 915–925.
2. Bai, C., Sen, P., Hofmann, K., Ma, L., Goebel, M., Harper, J.W., and Elledge, S.J. (1996). SKP1 connects cell cycle regulators to the ubiquitin proteolysis machinery through a novel motif, the F-box. *Cell* 86, 263–274.
3. Skowyra, D., Craig, K.L., Tyers, M., Elledge, S.J., and Harper, J.W. (1997). F-box proteins are receptors that recruit phosphorylated substrates to the SCF ubiquitin-ligase complex. *Cell* 91, 209–219.
4. Feldman, R.M., Correll, C.C., Kaplan, K.B., and Deshaies, R.J. (1997). A complex of Cdc4p, Skp1p, and Cdc53p/cullin catalyzes ubiquitination of the phosphorylated CDK inhibitor Sic1p. *Cell* 91, 221–230.
5. Tyers, M., and Jorgensen, P. (2000). Proteolysis and the cell cycle: with this RING I do thee destroy. *Curr. Opin. Genet. Dev.* 10, 54–64.

6. Deshaies, R.J. (1999). SCF and cullin/ring H2-based ubiquitin ligases. *Annu. Rev. Cell Dev. Biol.* **15**, 435–467.
7. Schulman, B.A., Carrano, A.C., Jeffrey, P.D., Bowen, Z., Kinnucan, E.R., Finnin, M.S., Elledge, S.J., Harper, J.W., Pagano, M., and Pavletich, N.P. (2000). Insights into SCF ubiquitin ligases from the structure of the Skp1-Skp2 complex. *Nature* **408**, 381–386.
8. Hershko, A., and Ciechanover, A. (1998). The ubiquitin system. *Annu. Rev. Biochem.* **67**, 425–479.
9. Strohmaier, H., Spruck, C.H., and Kaiser, P., Won, K.A., Sangfelt, O., and Reed, S.I. (2001). Human F-box protein hCdc4 targets cyclin E for proteolysis and is mutated in a breast cancer cell line. *Nature* **413**, 316–322.
10. Koepp, D.M., Schaefer, L.K., Ye, X., Keyomarsi, K., Chu, C., Harper, J.W., and Elledge, S.J. (2001). Phosphorylation-dependent ubiquitination of cyclin E by the SCF^{Fbw7} ubiquitin ligase. *Science* **294**, 173–177.
11. Kaplan, K.B., Hyman, A.A., and Sorger, P.K. (1997). Regulating the yeast kinetochore by ubiquitin-dependent degradation and Skp1p-mediated phosphorylation. *Cell* **91**, 491–500.
12. Russell, I.D., Grancell, A.S., and Sorger, P.K. (1999). The unstable F-box protein p58-Ctf13 forms the structural core of the CBF3 kinetochore complex. *J. Cell Biol.* **145**, 933–950.
13. Galan, J.M., Wiederkehr, A., Seol, J.H., Haguenaue-Tsapis, R., Deshaies, R.J., Riezman, H., and Peter, M. (2001). Skp1p and the F-box protein Rcy1p form a non-SCF complex involved in recycling of the SNARE Snc1p in yeast. *Mol. Cell. Biol.* **21**, 3105–3117.
14. Seol, J.H., Shevchenko, A., and Deshaies, R.J. (2001). Skp1 forms multiple protein complexes, including RAVE, a regulator of V-ATPase assembly. *Nat. Cell Biol.* **3**, 384–391.
15. Altschul, S.F., Madden, T.L., Schaffer, A.A., Zhang, J., Zhang, Z., Miller, W., and Lipman, D.J. (1997). Gapped BLAST and PSI-BLAST: a new generation of protein database search programs. *Nucleic Acids Res.* **25**, 3389–3402.
16. Liang, Y., Chen, H., Asher, J.H., Chang, C.-C., and Friedman, T.B. (1997). Human inner ear *OCP2* cDNA maps to 5q22–5q35.2 with related sequences on chromosomes 4p16.2–4p14, 5p13–5p22, 7pter-q22, 10 and 12p13–12qter. *Gene* **184**, 163–167.
17. Demetrick, D.J., Zhang, H., and Beach, D.H. (1996). Chromosomal mapping of the genes for the human CDK2/cyclin A-associated proteins p19 (SKP1A and SKP1B) and p45 (SKP2). *Cytogenet. Cell Genet.* **73**, 104–107.
18. Saitou, N., and Nei, M. (1987). The neighbor-joining method: a new method for reconstructing phylogenetic trees. *Mol. Biol. Evol.* **4**, 406–425.
19. Felsenstein, J. (1981). Evolutionary trees from DNA sequences: a maximum likelihood approach. *J. Mol. Evol.* **17**, 368–376.
20. Lyons-Weiler, J., and Hoelzer, G.A. (1997). Escaping from the Felsenstein zone by detecting long branches in phylogenetic data. *Mol. Phylogenet. Evol.* **8**, 375–384.
21. Fire, A., Xu, S., Montgomery, M.K., Kostas, S.A., Driver, S.E., and Mello, C.C. (1998). Potent and specific genetic interference by double-stranded RNA in *Caenorhabditis elegans*. *Nature* **391**, 806–811.
22. Gonczy, P., Echeverri, G., Oegema, K., Coulson, A., Jones, S.J., Copley, R.R., Duperon, J., Oegema, J., Brehm, M., Cassin, E., et al. (2000). Functional genomic analysis of cell division in *C. elegans* using RNAi of genes on chromosome III. *Nature* **408**, 331–336.
23. Parrish, S., Fleenor, J., Xu, S., Mello, C., and Fire, A. (2000). Functional anatomy of a dsRNA trigger. Differential requirement for the two trigger strands in RNA interference. *Mol. Cell* **6**, 1077–1087.
24. Sulston, J.E., Schierenberg, E., White, J.G., and Thomson, J.N. (1983). The embryonic cell lineage of the nematode *Caenorhabditis elegans*. *Dev. Biol.* **100**, 64–119.
25. Kipreos, E.T., Lander, L.E., Wing, J.P., He, W.W., and Hedgecock, E.M. (1996). *cul-1* is required for cell cycle exit in *C. elegans* and identifies a novel gene family. *Cell* **85**, 829–839.
26. Reinke, V., Smith, H.E., Nance, J., Wang, J., Van Doren, C., Begley, R., Jones, S.J., Davis, E.B., Scherer, S., Ward, S., et al. (2000). A global profile of germline gene expression in *C. elegans*. *Mol. Cell* **6**, 605–616.
27. Piano, F., Schetter, A.J., Mangone, M., Stein, L., and Kemphues, K.J. (2000). RNAi analysis of genes expressed in the ovary of *Caenorhabditis elegans*. *Curr. Biol.* **10**, 1619–1622.
28. Hill, A.A., Hunter, C.P., Tsung, B.T., Tucker-Kellogg, G., and Brown, E.L. (2000). Genomic analysis of gene expression in *C. elegans*. *Science* **290**, 809–812.
29. Ashcroft, N.R., Srayko, M., Kosinski, M.E., Mains, P.E., and Golden, A. (1999). RNA-mediated interference of a *cdc25* homolog in *Caenorhabditis elegans* results in defects in the embryonic cortical membrane, meiosis, and mitosis. *Dev. Biol.* **206**, 15–32.
30. Feng, H., Zhong, W., Punkosdy, G., Gu, S., Zhou, L., Seabolt, E.K., and Kipreos, E.T. (1999). CUL-2 is required for the G1-to-S-phase transition and mitotic chromosome condensation in *Caenorhabditis elegans*. *Nat. Cell Biol.* **1**, 486–492.
31. Tabara, H., Sarkissian, M., Kelly, W.G., Fleenor, J., Grishok, A., Timmons, L., Fire, A., and Mello, C.C. (1999). The *rde-1* gene, RNA interference, and transposon silencing in *C. elegans*. *Cell* **99**, 123–132.
32. Jones, A.R., Francis, R., and Schedl, T. (1996). GLD-1, a cytoplasmic protein essential for oocyte differentiation, shows stage- and sex-specific expression during *Caenorhabditis elegans* germline development. *Dev. Biol.* **180**, 165–183.
33. Zetka, M.C., Kawasaki, I., Strome, S., and Muller, F. (1999). Synapsis and chiasma formation in *Caenorhabditis elegans* require HIM-3, a meiotic chromosome core component that functions in chromosome segregation. *Genes Dev.* **13**, 2258–2270.
34. Ward, S., Roberts, T.M., Strome, S., Pavalko, F.M., and Hogan, E. (1986). Monoclonal antibodies that recognize a polypeptide antigenic determinant shared by multiple *Caenorhabditis elegans* sperm-specific proteins. *J. Cell Biol.* **102**, 1778–1786.
35. Fraser, A.G., Kamath, R.S., Zipperlen, P., Martinez-Campos, M., Souhrmann, M., and Ahringer, J. (2000). Functional genomic analysis of *C. elegans* chromosome I by systematic RNA interference. *Nature* **408**, 325–330.
36. Kipreos, E.T., and Pagano, M. (2000). The F-box protein family. *Genome Biol.* **1**, 3002.1–3002.7.
37. Michel, J.J., and Xiong, Y. (1998). Human CUL-1, but not other cullin family members, selectively interacts with SKP1 to form a complex with SKP2 and cyclin A. *Cell Growth Differ.* **9**, 435–449.
38. Church, D.L., Guan, K.L., and Lambie, E.J. (1995). Three genes of the MAP kinase cascade, *mek-2*, *mpk-1/sur-1* and *let-60 ras*, are required for meiotic cell cycle progression in *Caenorhabditis elegans*. *Development* **121**, 2525–2535.
39. Francis, R., Barton, M.K., Kimble, J., and Schedl, T. (1995a). *gld-1*, a tumor suppressor gene required for oocyte development in *Caenorhabditis elegans*. *Genetics* **139**, 607–630.
40. Francis, R., Maine, E., and Schedl, T. (1995b). Analysis of the multiple roles of *gld-1* in germline development: interactions with the sex determination cascade and the *glp-1* signaling pathway. *Genetics* **139**, 607–630.
41. Karashima, T., Sugimoto, A., and Yamamoto, M. (2000). *Caenorhabditis elegans* homologue of the human azoospermia factor DAZ is required for oogenesis but not for spermatogenesis. *Development* **127**, 1069–1079.
42. Geles, K.G., and Adam, S.A. (2001). Germline and developmental roles of the nuclear transport factor importin alpha3 in *C. elegans*. *Development* **128**, 1817–1830.
43. MacQueen, A.J., and Villeneuve, A.M. (2001). Nuclear reorganization and homologous chromosome pairing during meiotic prophase require *C. elegans chk-2*. *Genes Dev.* **15**, 1674–1687.
44. Dernburg, A.F., McDonald, K., Moulder, G., Barstead, R., Dresser, M., and Villeneuve, A.M. (1998). Meiotic recombination in *C. elegans* initiates by a conserved mechanism and is dispensable for homologous chromosome synapsis. *Cell* **94**, 387–398.
45. Kuwabara, P.E., and Coulson, A. (2000). RNAi—prospects for a general technique for determining gene function. *Parasitol. Today* **16**, 347–349.
46. Thompson, J.D., Higgins, D.G., and Gibson, T.J. (1994). CLUSTAL W: improving the sensitivity of progressive multiple sequence alignment through sequence weighting, position-specific gap penalties and weight matrix choice. *Nucleic Acids Res.* **22**, 4673–4680.
47. James, P., Halladay, J., and Craig, E.A. (1996). Genomic libraries

- and a host strain designed for highly efficient two-hybrid selection in yeast. *Genetics* **144**, 1425–1436.
48. Janssen, K. (1995). *Current Protocols in Molecular Biology* (Boston: John Wiley & Sons).
 49. Schedl, T. (1997). Developmental genetics of the germ line. In *C. elegans* II. D.L. Riddle, T. Blumenthal, B.J. Meyer, and J.R. Priess, eds. (Cold Spring Harbor, NY: Cold Spring Harbor Laboratory Press), pp. 241–269.
 50. Grant, B., and Hirsh, D. (1999). Receptor-mediated endocytosis in the *Caenorhabditis elegans* oocyte. *Mol. Biol. Cell* **10**, 4311–4326.